2020

Seismic Performance of Modular Steel-Braced Frames Utilizing Superelastic Shape Memory Alloy Bolts in the Vertical Module Connections

Papia Sultana
Western University

Maged A. Youssef
Western University, youssef@uwo.ca

Seismic performance of modular steel braced frames utilizing superelastic shape memory alloy bolts in the vertical module connections

Papia Sultana[a] and Maged A. Youssef[b]

Abstract: In modular construction, individual modules are constructed at a controlled industrial environment before being transported to site. They are then connected horizontally and vertically to form a structure. The vertical connections can be achieved by welding or bolting the columns of stacked modules. This study investigates the seismic performance of modular steel braced frames (MSBFs) connected vertically using superelastic shape memory alloy (SMA) bolts. The study also identifies the required locations of SMA connections, in a typical MSBF, to optimize its seismic performance in terms of maximum inter-storey drift (MID), maximum residual inter-storey residual drift (MRID), and damage scheme.

Keywords: Modular steel building, Shape memory alloy, Bolted connection, Dynamic analysis, Inter-storey drift, Residual drift.

[a] PhD Candidate, Western University, Civil and Environmental Engineering, London, ON, Canada N6A 5B9, Email: psultana@uwo.ca.

[b] **Corresponding Author**, Professor, Western University, Civil and Environmental Engineering, London, ON, Canada N6A 5B9, Email: youssef@uwo.ca, Tel.: 519-661-2111 Ext. 88661.

1.0 INTRODUCTION

Modular steel buildings (MSBs) are widely used for one-to-six storey buildings, where repetitive units are required, such as in schools, office buildings, hospitals, student residences, and military accommodations. The demand for MSBs is increasing because of their high quality, fast on-site installation, and lower cost of construction. They differ from regular steel construction in terms of detailing requirements and method of construction. Rectangular or square hollow steel sections (RHS/SHS) are commonly used as column sections in MSBs. The columns of stacked modules are connected vertically either by field welding or bolting, as shown in Figure 1. For a corner column, welding can only be achieved at the exterior faces. Considering bolted connections, access holes with a 50 mm diameter are needed to install the bolts [1].

Lawson and Richards [2] presented a review of modular technologies and proposed a design method for high-rise-modular buildings, which accounts for installation and construction tolerance. However, they did not discuss their seismic behaviour. Annan et al. [3-5] investigated the seismic performance of modular steel braced frames (MSBFs) that utilized field welding in their vertical connections. The seismic performance of MSBFs was found to be significantly different from regular steel braced frames due to the existence of ceiling beams, the eccentricity developed at the joints as the braces do not intersect at a single working point, and the allowed rotation at the semi-rigid welded connections between the columns of a module and the ones above or below them.

During 1994 Northridge and 1995 Kobe earthquakes, fracture of welded beam to column connections was widely observed due to the degraded base material properties after welding, the inherent low toughness of weld filler metals, and the hidden defects in the connection [6]. To

eliminate this undesirable failure, bolted connections were recommended to replace welded connections [7-9]. Frames employing properly designed bolted connections are capable of undergoing an extensive inelastic response, with plastic hinges forming either in the connections or in the beams [6]. To force the inelastic behaviour to occur within the connection, their plastic moment should be set as a fraction of that of the connected framing elements [6].

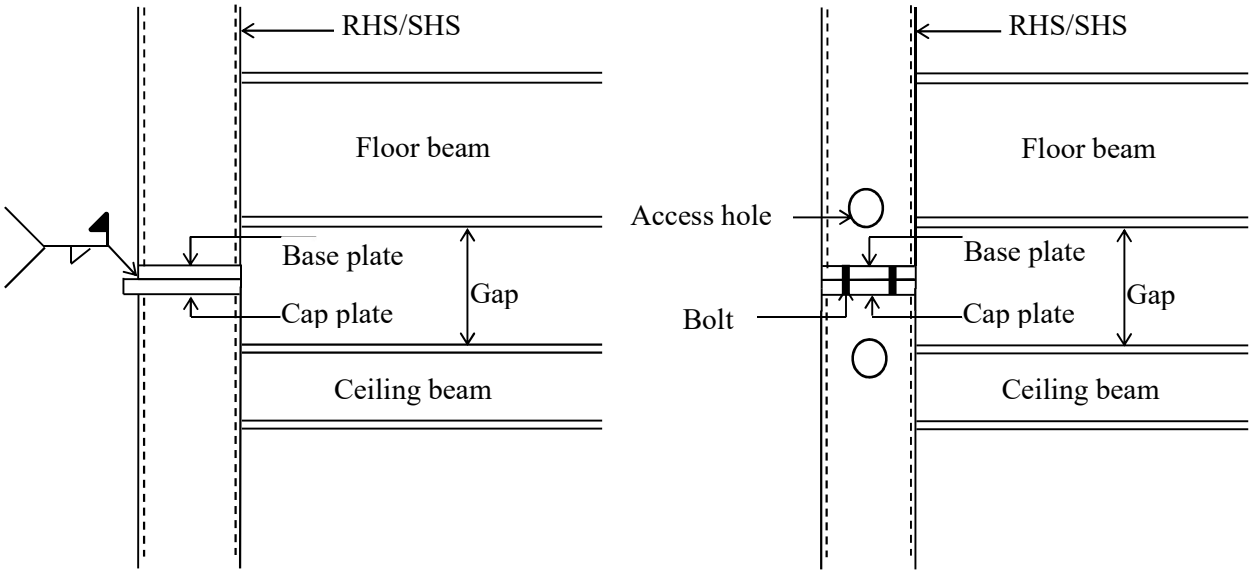

a) Welded connection b) Bolted connection

Figure 1: Vertical connections between upper and lower modules.

Residual drifts affect the decision to repair or demolish a seismically damaged structure [10]. Superelastic shape memory alloys (SMA) attracted the attention of researchers in recent years as a potential solution for this problem because of its self-centering as well as energy dissipation features. The most studied alloy is composed of Nickel and Titanium (NiTi) [11]. Superelasticity is the ability of the alloy to experience relatively high inelastic strains, and then recover its original shape when the load is removed. Researchers investigated the seismic performance of bolted beam-to-column connections incorporating superelastic SMA material and found that they have

excellent re-centering capability as well as moderate energy dissipation [12-16]. The global seismic performance of steel moment resisting frames employing SMA connections was studied by DesRoches et al. [17] and Sultana and Youssef [18]. SMA connections improved the seismic performance in terms of maximum inter-storey drift (MID), maximum residual inter-storey drift (MRID), and damage scheme [18].

Although few research studies addressed the use of SMA bolts in steel moment resisting frames, previous research did not explore the use of superelastic SMA in the vertical connections of MSBs. This study investigates the seismic performance of MSBFs that utilize high strength steel and/or superelastic SMA bolts in their vertical connections. The possibility to use SMA connections at selected locations of the frame, and, thus reduce the associated costs is also investigated.

2.0 MODULAR STEEL BRACED FRAMES

The six-storey modular steel building, located in Vancouver, British Columbia, Canada, and designed by Annan et al. [4] according to the Canadian standard CSA-S16-01 [19] and the National Building Code of Canada [20], was selected as a case study. Annan et al. [4] estimated the seismic loads using the NBCC equivalent static load approach [20], which is based on uniform hazard values corresponding to a 2% in 50-year probability of exceedance. The building was assumed to be founded on a very dense soil (site class C), having an average shear wave velocity of 360 m/s to 760 m/s. The overstrength and ductility factors were equal to 1.3 and 3.0, respectively. The plan and elevation of the MSB are shown in Figure 2. Each floor consists of six modular units, which are connected horizontally. Lateral forces are resisted by the external braced frames. The lateral response in the N-S direction is considered in this study, which is controlled by two-identical

braced-frames (Fig. 2b). Details of the MSB design are given by Annan et al. [4]. Floor and ceiling beams are W250×33 and W100×19, respectively. In this paper, braces are replaced with buckling restrained braces (BRB). X-shaped steel braces can be restrained using concrete panels [21] or steel elements. Sections for the columns and the braces are given in Table 1. The connections between beams and columns, and braces and gusset plates are achieved by welding. A clearance of 150 mm is allowed between floor beams and ceiling beams to install a fire protective layer. The welded vertical connections between the modules, which were designed by Annan et al. [4], are replaced in this paper by bolted connections. Frame 1, which utilizes 4-M30 high strength steel bolts in each vertical connection. The bolts have been designed such that the lateral performance of the frame is governed by yielding of the braces. The diameter and number of the bolts remained unchanged for all of the vertical connections to match construction practices. The thickness of the base and cap plates was 20 mm, which ensured rigid plate behaviour.

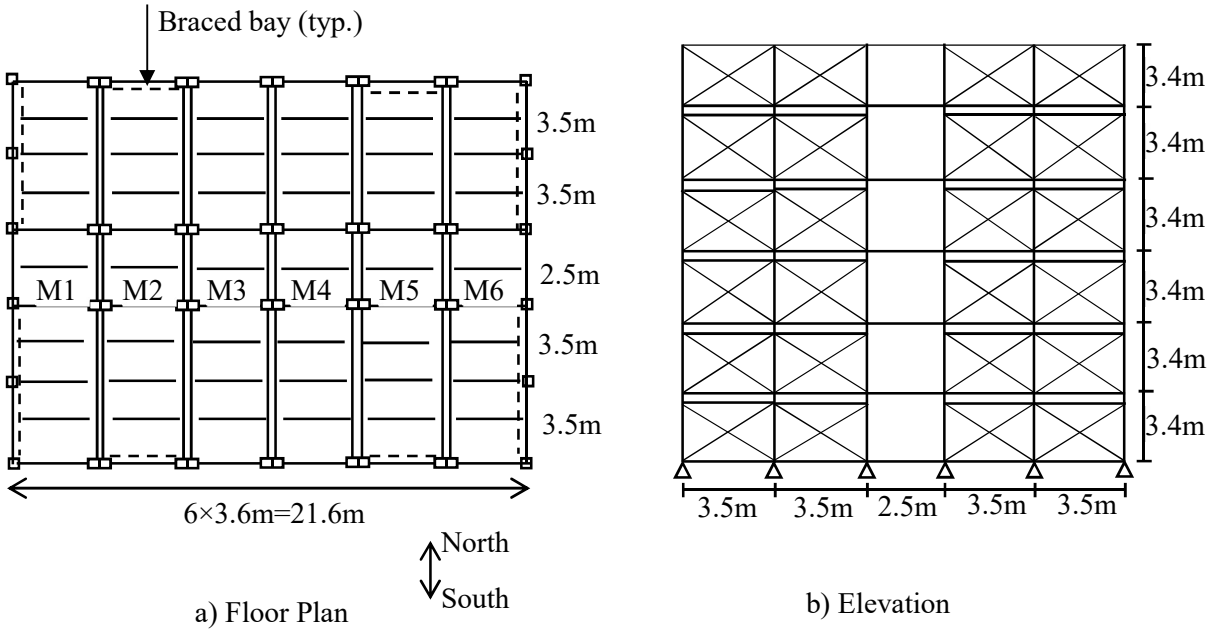

Figure 2 Six-storey modular steel braced frames

Vertical connections of Frame 1 were redesigned by replacing some of the high strength steel bolts with M24 superelastic SMA bolts. The SMA material properties used in this study are provided in Table 2. The capacity provided by the SMA bolts is about 40% of that by the high strength bolts. This ratio is chosen based on preliminary analysis to ensure that the austenite-to-martensite starting stress is reached and the limit for superelastic strains is not exceeded. It is expected that using SMA connections between all modules (Frame 2) will minimize the residual drifts. To examine the effects of higher modes of vibrations, and reduce the cost associated with using SMA bars, Frames 3 to 6 are examined. The locations of the SMA vertical connections are shown in Figure 3 and they are between: (1) all modules (Frame 2), (2) 1st and 2nd storey modules (Frame 3), (3) 1st and 2nd as well as 2nd and 3rd storey modules (Frame 4), (4) 1st and 2nd as well as 3rd and 4th storey modules (Frame 5), (5) 1st and 2nd as well as 4th and 5th storey modules (Frame 6).

Table 1: Section properties of the MSBF

Storey	Column Sections	Area of Brace Core (mm^2)
Storey 6	HS 102×102×6	1200
Storey 5	HS 178×178×6	2100
Storey 4	HS 203×203×10	2100
Storey3	HS 305×305×10	2100
Storey 2	HS 305×305×13	2100
Storey 1	HS 305×305×13	2100

Table 2: Material properties of SMA

Modulus of elasticity, E	40,000 MPa
Austenite-to-martensite starting stress	524 MPa
Austenite-to-martensite finishing stress	850 MPa
Martensite-to-austenite starting stress	450 MPa
Martensite-to-austenite finishing stress	200 MPa
Superelastic strain limit	6%

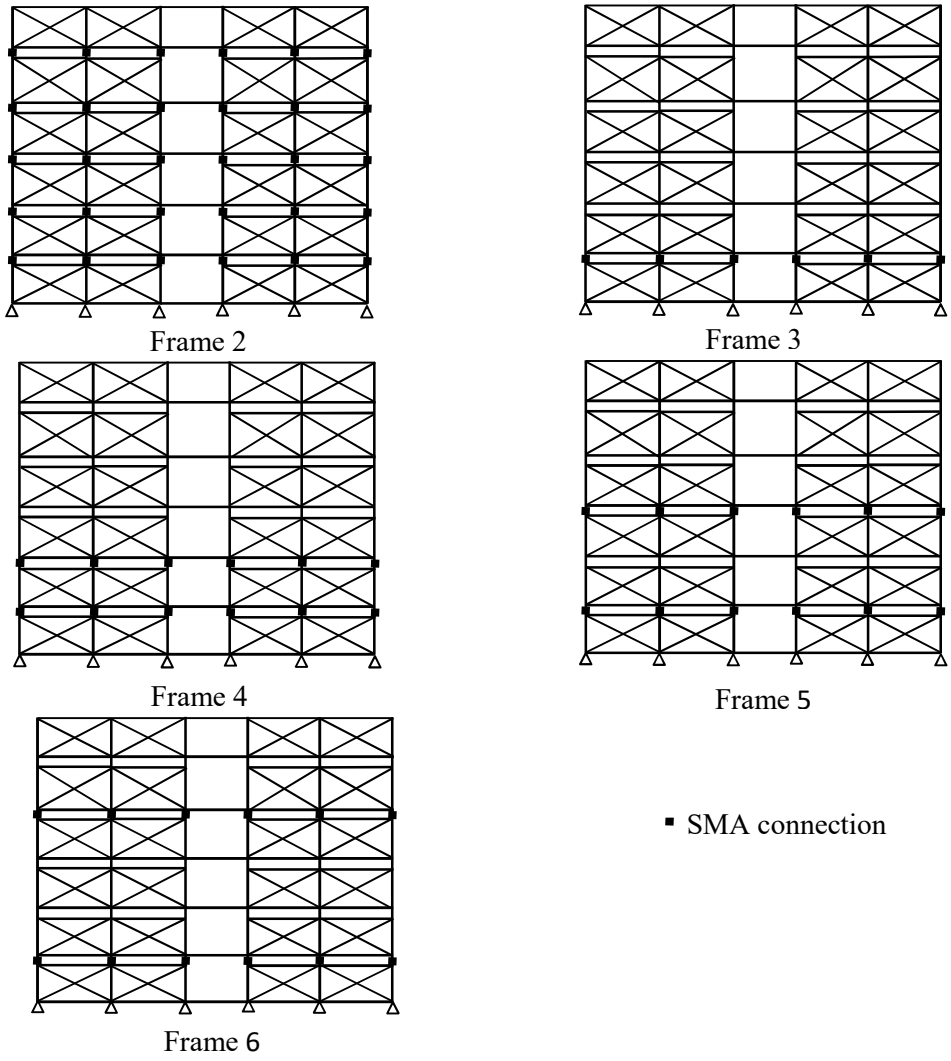

Figure 3: Locations of SMA connections

3.0 FINITE ELEMENT MODELING OF MSBFS

A nonlinear two-dimensional model of the MSBF was developed using the software SeismoStruct [22]. The model was based on the fibre element approach where each fibre was assigned a uniaxial stress–strain relationship. The beams and columns were modelled using force-based inelastic frame elements. The distributed dead load and 25% of the live load were applied to the beams. The

mass of each floor was converted into lumped masses at the joints. Careful attention was made to the unique detailing of the MSB. Specific modeling assumptions are given below.

1) As beams and columns were assumed to be connected by direct welding, rigid beam-to-column connections were utilized.
2) The steel braces were modelled using inelastic truss elements. Buckling behaviour was not modelled as braces were assumed to be buckling restrained.
3) Inelastic truss elements and compression only link elements were utilized to model the bolts and bearing behavior of the vertical connections, respectively.
4) The base and cap plates were modelled using rigid elements to simulate the rigid plate behaviour.
5) The shear deformations of the bolts were ignored and the horizontal displacements of points along the rigid element representing the base plates were constrained to the matching points in the cap plates.
6) Equivalent viscous damping of 5% was assumed to model the non-hysteretic damping.

Figure 4 shows the finite element model of the vertical connections of the MSBFs. The P-Δ effect is accounted for in the analysis. The material model parameters for the steel beams, columns and braces were as follows: yield stress of 350 N/mm^2, elastic modulus of 200 kN/mm^2, and strain hardening of 1%. The yield strength of the steel bolts was 780 MPa.

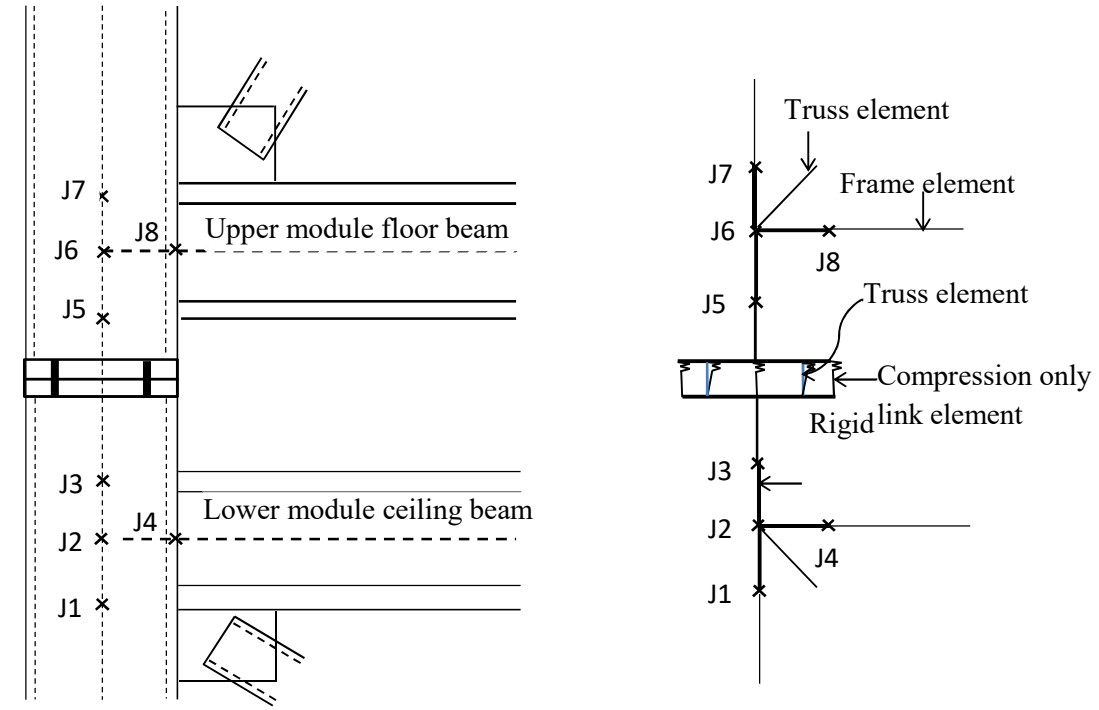

Vertical connection representation Model representation

Figure 4: Finite element model of MSBF

3.1 Validation of FE modeling technique

Three different finite element models were used to validate the modeling technique. They covered the modeling aspects that relate to: (1) the unique details of MSBF, (2) the vertical bolted connections between the modules, and (3) superelasticity and energy dissipation of SMA bolts. Details of these models are discussed in this section.

The one-storey MSBF tested by Annan et al. [3] under cycling loading was modeled. Figures 5 and 6 show details of the frame and the corresponding FE model. Member M1 models a vertical distance of 150 mm that accounts for the fire proofing clearance. The modules were connected vertically by field welding at the outer faces of the columns. This connection allows independent

rotations of the upper and lower modules. Thus, the vertical joint, j5, was simulated using a pin connection to allow this independent rotation. Figure 7 compares the experimental and analytical results. The maximum base shear predicted by the FE analysis is lower than the experimental one by 6.67%. The model was also able to accurately capture the energy dissipation characteristics and the residual drift values.

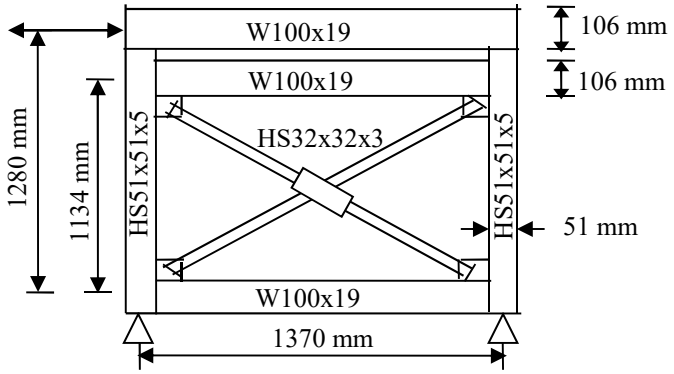

Figure 5: Geometry of MSBF tested by Annan et al. [3]

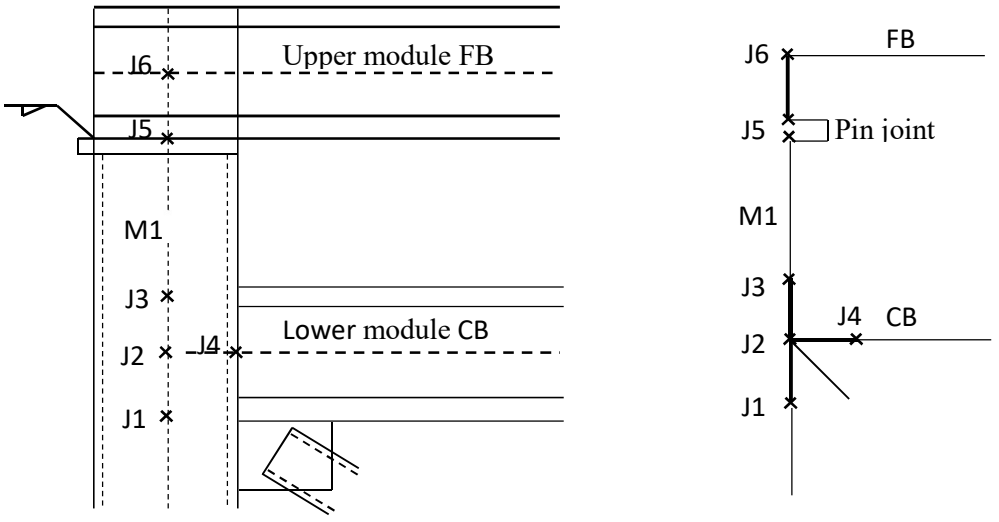

Vertical connection representation Model representation

Figure 6: Model of vertical connection of MSBF

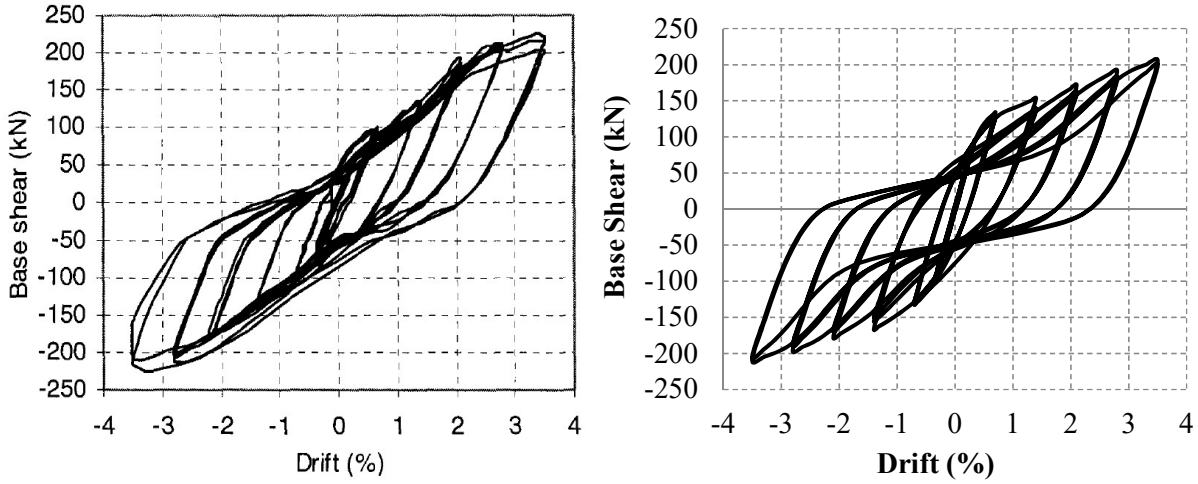

a) Experimental result [3] b) Numerical simulation

Figure 7: Comparison of experimental and numerical results

Wheeler et al. [23] conducted an experimental program to investigate the moment capacity of end-plate connections in rectangular/square hollow sections (RHS/SHS). A simply supported beam spliced at mid-span section was subjected to a four-point bending test. The beam section was a square hollow section, SHS 150×150×9, and was spliced at mid-span using 4-M20 bolts, as shown in Figure 8. The end plates were modeled using frame elements that were rigid within the hollow section and represented the nonlinear plate stiffness outside the section. Inelastic truss elements modeled the steel bolts. Figure 9 shows a comparison of the numerical and experimental moment-rotation behaviour of the connection and demonstrates the accuracy of the end-plate model in capturing the connection behaviour. The numerical ultimate moment capacity of the connection is 1.29% greater than the experimental value. Failure of the connection was due to tensile failure of the bolts, which agreed with the experimental results.

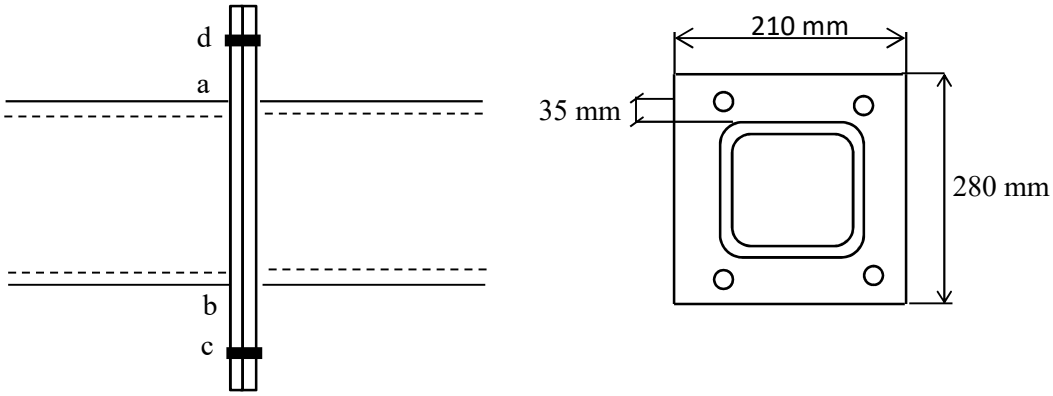

a) Beam splices connection

b) End plate layout

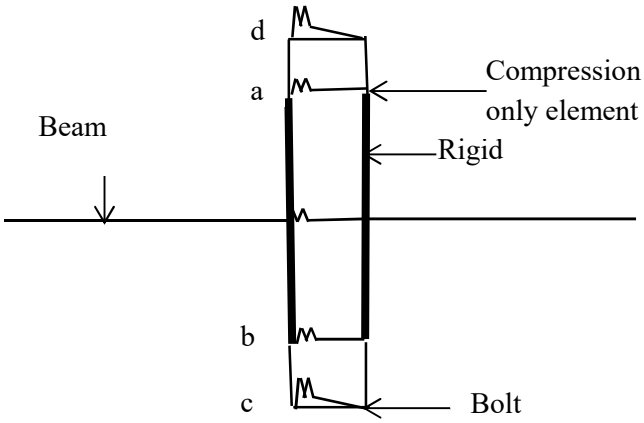

c) FE model

Figure 8: Bolted end-plate connection

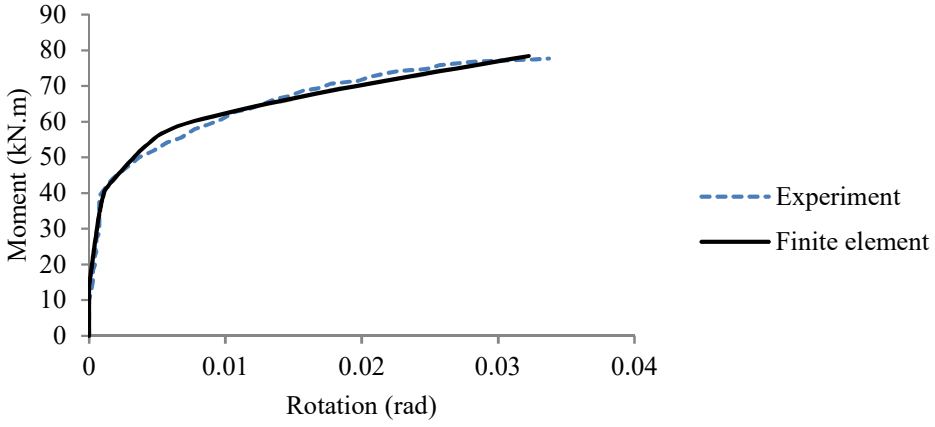

Figure 9: Comparison of experimental and simulated moment rotation behaviour of bolted connection

The interior beam-column connection that utilized superelastic SMA bars and tested by Speicher et al. [16] was modeled by Sultana and Youssef [18]. The superelastic behaviour of SMA material was modeled using the uniaxial material model proposed by Auricchio and Sacco [24] and programmed by Fugazza [25]. The connection model was found to be capable of predicting the moment-rotation response, energy dissipation, and residual deformations with adequate accuracy [18].

4.0 SEISMIC PERFORMANCE OF MSBF WITH STEEL BOLTED VERTICAL CONNECTION (FRAME 1)

Frame 1, the MSBF equipped with steel bolted connections, was modeled using the validated modelling technique. Eigen value analysis resulted in first and second natural periods of vibrations of 0.55 second and 0.19 second, respectively. Five different ground motions, which are given in Table 3, were then selected from PEER ground motion database [26]. The elastic response spectra of these unscaled ground motions considering 5% damping is shown in Figure 10. The seismic intensity is expressed in terms of the spectral acceleration at the first period of vibration [Sa(T1, 5%)]. Incremental dynamic analyses (IDA) were performed by scaling the ground motions to different intensities. IDA analyses were stopped at an earthquake intensity of 1.5g or failure of any of the steel elements, which was assumed when its strains reach 0.06. Results of the IDA at three different intensities are discussed in this section.

Table 3: Characteristics of ground motions

Earthquake	Year	Ms magnitude	Station	PGA(g)
Northridge	1994	6.7	Arleta-Nordhoff	0.344
Superstition hill-02	1987	6.5	Parachute Test Site	0.432
Loma Prieta	1989	7.1	Capitola	0.529
Tabas	1978	6.9	Tabas	0.852
San Fernando	1971	6.6	Pacoima dam	1.230

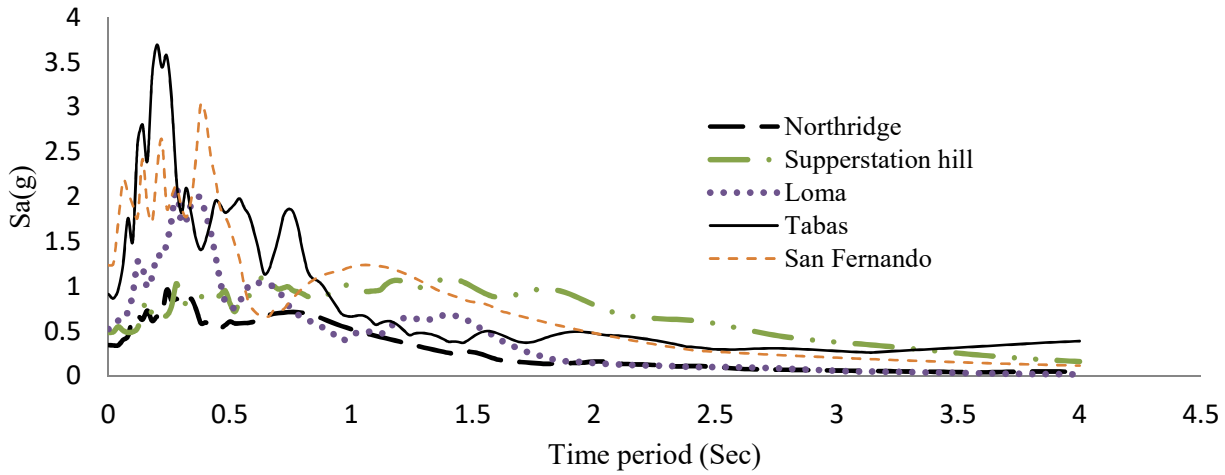

Figure 10: Elastic response spectral acceleration

MID and MRID values of Frame 1 at different seismic intensities are given in Table 4. Their values reached 0.78% and 0.14%, respectively. MID occurred at the upper stories at seismic intensities lower than 1.2g. However, at higher seismic intensities, it occurred at the first storey leading to a soft first storey failure mechanism. The storey experiencing the MID was not always the storey experiencing the MRID. The 1st storey experienced the MRID for twelve of the conducted fifteen analyses. Figure 11 shows the damage distribution of Frame 1. The beams in the unbraced bays yielded in all cases. Yielding of the braces was observed in the first four stories due to Tabas (1.5g), Northridge (1.3g) and San Fernando (1.5g) earthquakes, and in the first three stories due to

Loma (1.3g) and Superstition Hill (1.5g) earthquakes. Yielding of a 1st storey column was also observed in case of Tabas, Northridge, and Superstition Hill earthquakes. The first floor experienced more damage when compared to the remaining floors as was reflected in the large inelastic brace deformations as well as column yielding.

Table 4 MID and MRID of Frame 1 at different intensity of ground motions

Earthquakes	Sa (T1,5%)	MID%	MRID%
Northridge	1.0g	0.54 (4th storey)	0.01 (6th storey)
	1.2g	0.62 (5th storey)	0.03 (1st storey)
	1.3g	0.67 (1st storey)	0.10 (1st storey)
Superstition hill	1.0g	0.46 (4th storey)	0.01(2nd storey)
	1.2g	0.54 (4th storey)	0.03 (1st storey)
	1.5g	0.78 (1st storey)	0.14 (1st storey)
Loma	1.0g	0.45 (3rd storey)	0.02 (1st storey)
	1.2g	0.58 (1st storey)	0.07 (1st storey)
	1.3g	0.68 (1st storey)	0.07 (1st storey)
Tabas	1.0g	0.58 (6th storey)	0.01 (6th storey)
	1.2g	0.67 (6th storey)	0.04 (1st storey)
	1.5g	0.74 (6th storey)	0.09 (1st storey)
San Fernando	1.0g	0.51 (6th storey)	0.01 (1st storey)
	1.2g	0.58 (6th storey)	0.03 (1st storey)
	1.5g	0.69 (1st storey)	0.02 (1st storey)

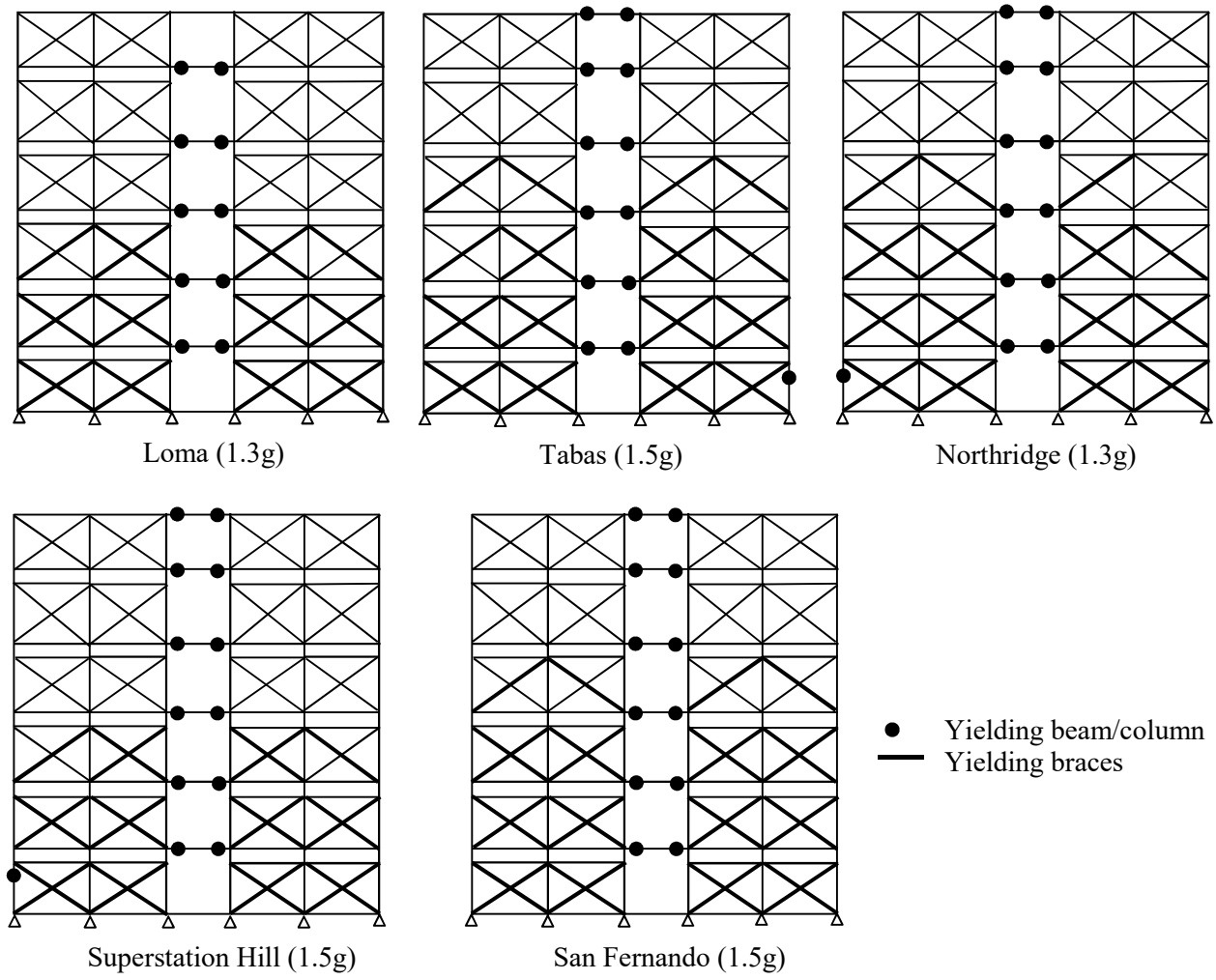

Figure 11: Damage distribution of Frame 1

5. SEISMIC PERFORMANCE OF MSBF EQUIPPED WITH SMA BOLTED VERTICAL CONNECTIONS

Eigen value analyses were performed for the frames with SMA bolted connections. The obtained first and second natural periods of vibrations were similar to those of Frame 1. Nonlinear dynamic time history analysis was performed considering the same ground motions at the same intensities for Frame 1. The values of MID and MRID of the different frames considering different earthquake

intensities are compared in Figures 12-16. Using SMA connections did not only change the values of MIDs and MRIDs, but also changed the locations of stories experiencing these values. The maximum values of MID (0.87%) and MRID (0.11%) were observed in Frame 2. The percentage difference between the observed MID and MRID for Frames 2 to 6 as compared to Frame 1 are presented in Table 5. The use of SMA bolts in the vertical connections increased the MID considering Northridge and Tabas earthquakes and reduced it considering San Fernando earthquake. The seismic intensity influenced the MID values. For example, in case of Superstition Hill earthquake, the MID of the SMA frames relative to Frame 1 increased with increasing the intensity from 1.0g to 1.2g and decreased at an intensity of 1.5g. The highest increase in MID (25.5%) occurred in Frame 2, whereas the highest reduction (15.5%) occurred in Frame 3. It is clear that the number of SMA connections, their locations, and the earthquake intensity affected the values of MIDs.

The MRIDs were significantly reduced by using SMA in vertical connections as shown in Figures 12 to 16. The reductions in MRID values were 91.5%, 82.9%, 87.1%, 85.6%, and 84.5% for Frames 2, 3 4, 5 and 6, respectively. The reduction of MRID depends on the number and the locations of SMA connections as well as the ground motion and its intensity. The reduction in the MRID in Frame 2 increased from 30.0% to 91.5%, when the intensity of Tabas earthquake increased from 1.0g to 1.5g.

The average values of the percentage changes of MID and MRID for the different SMA frames were also compared in Table 5. The influence of SMA bolts on reducing MRID is clear up to an earthquake intensity of 1.2g. The maximum average reduction (73.8%) occurred in Frame 4. At seismic intensity of 1.3g or more, the average reduction in MRID (46.1%) occurred in Frame 5.

Figure 17 compares the MRIDs at different earthquake intensities for the six different frames. Introducing SMA bolts significantly reduced MRID. The effect is more pronounced at seismic intensities greater than 1.0g.

Utilizing SMA at carefully chosen locations plays a vital role in reducing the residual drifts. At an intensity of 1.3g, using SMA bolts increased the MRID for the Frames 3 and 6 considering Northridge earthquake, and Frames 2, 3, 5, and 6 considering Loma earthquake. This highlights that using SMA at the wrong locations might worsen the seismic performance. Frame 4 showed better seismic performance as compared to the other SMA frames. Its MRID was reduced considering all seismic records with an average of 57.4%.

ID and RID distributions along building height are shown in Figures 18 to 22. It was observed that the IDs for Frames 2 to 6 were very similar; however, the RIDs were significantly different. Utilizing SMA in the vertical connections redistributed the seismic forces in the frame, and, thus significantly reduced the residual drifts of the 1st storey. However, this reduction was not pronounced in other storeys of the SMA frames.

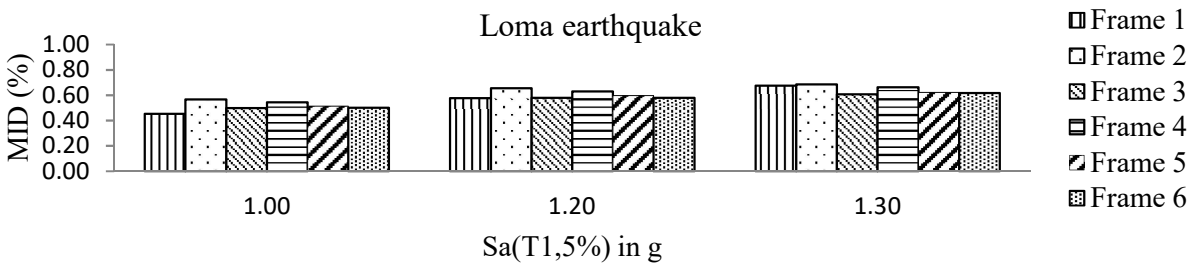

a) MID

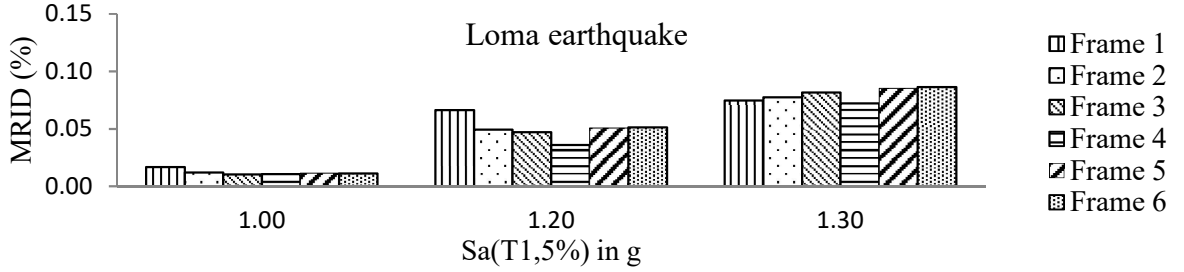

b) MRID

Figure 12: Drifts considering Loma earthquake

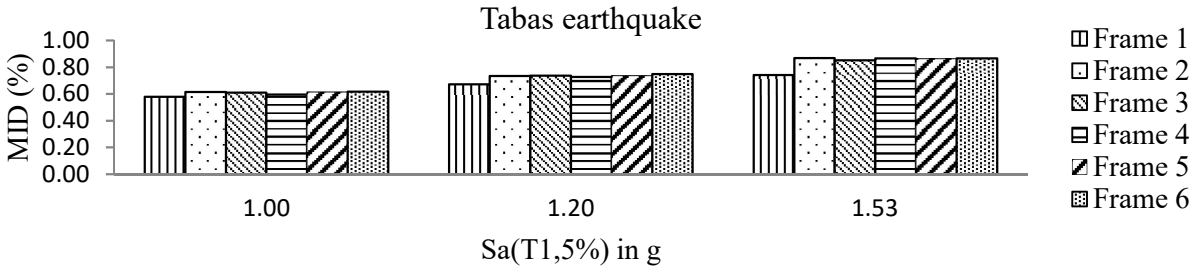

a) MID

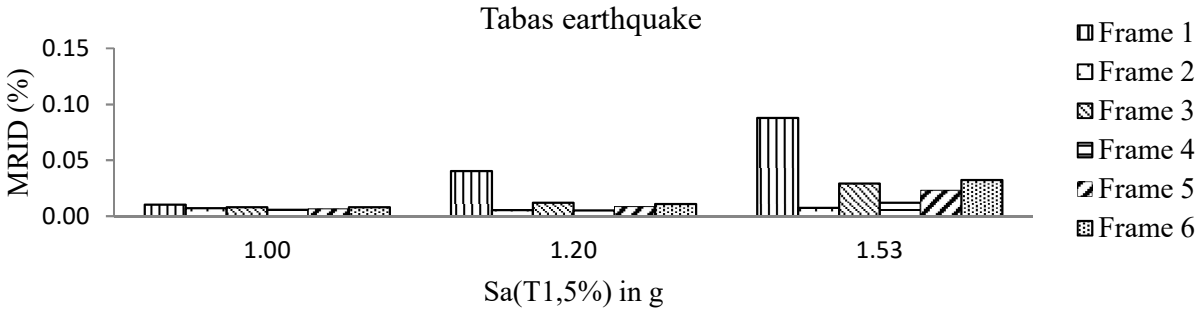

b) MRID

Figure 13: Drift considering Tabas earthquake

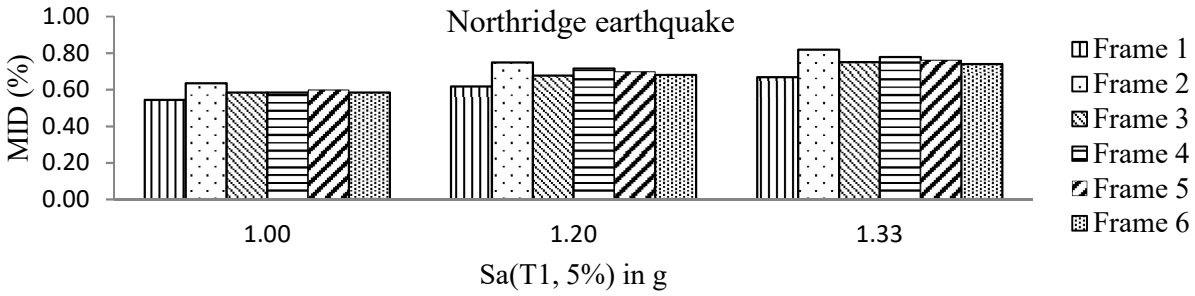

a) MID

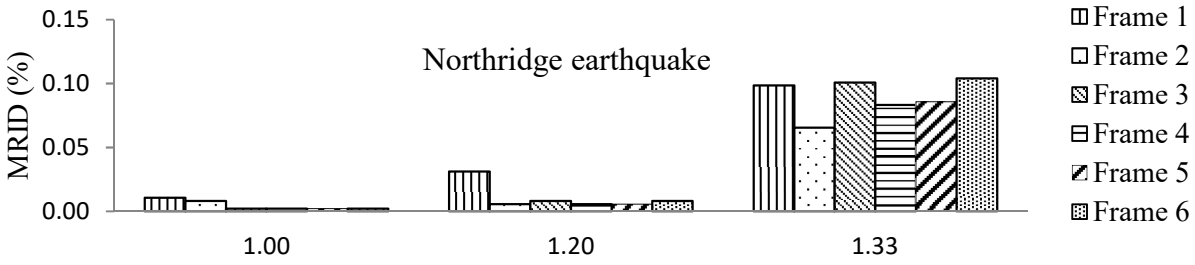

b) MRID

Figure 14: Drifts considering Northridge earthquake

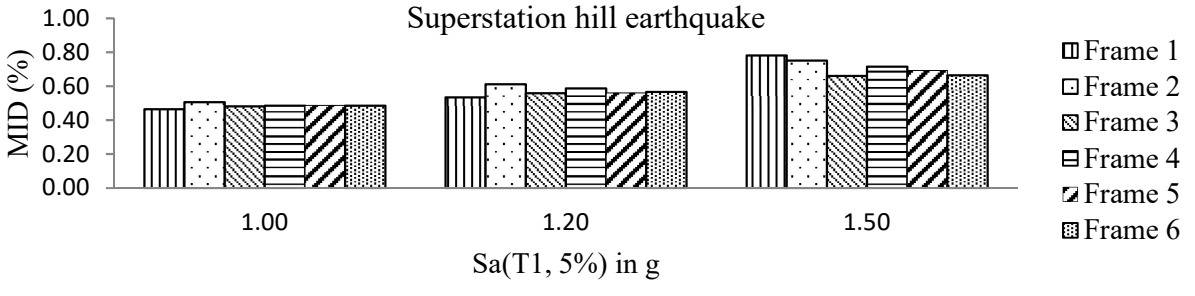

a) MID

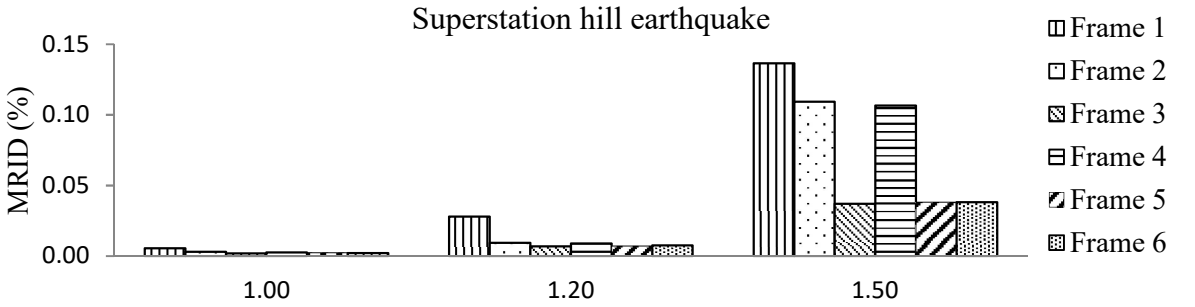

b) MRID

Figure 15: Drifts considering Superstition Hill earthquake

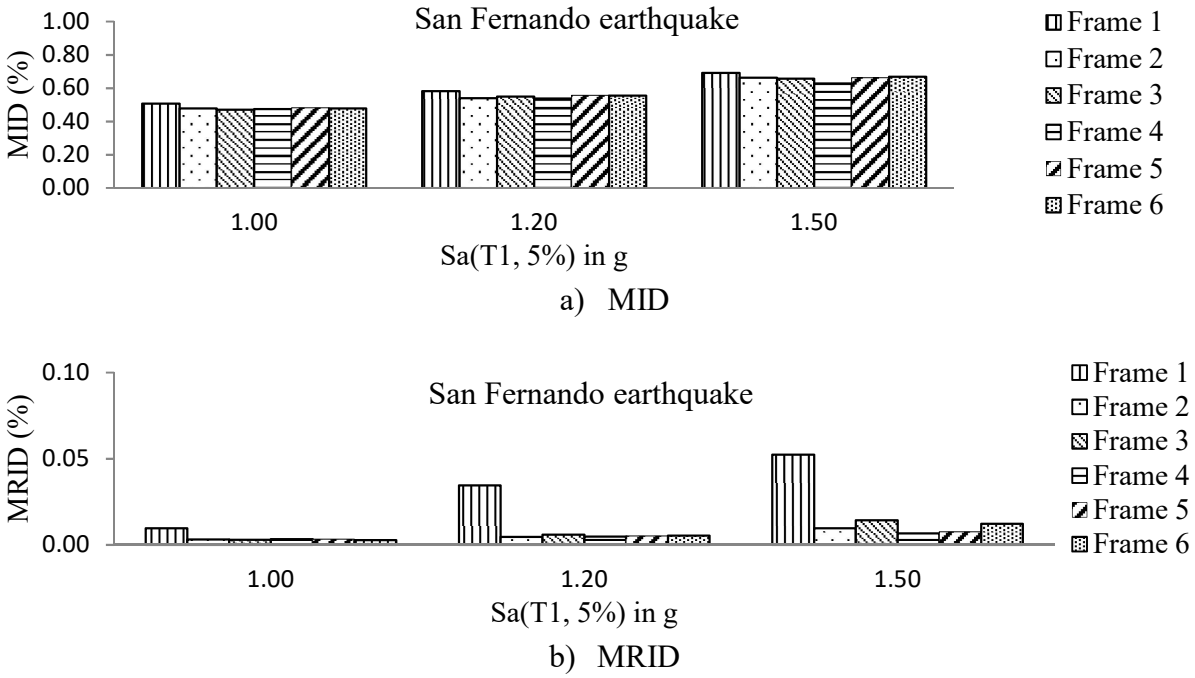

Figure 16: Drifts considering San Fernando earthquake

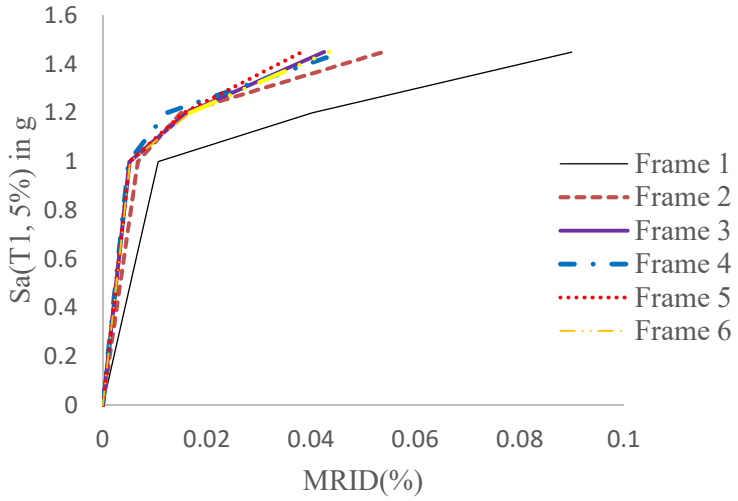

Figure 17: S_a (T1, 5%) versus MRID (%)

Table 5: Percentage change of MID and MRID of SMA frames

Ground motion	Intensity	Frame 2		Frame 3		Frame 4		Frame 5		Frame 6	
	Sa(T1,5%) in g	MID change (%)	MRID change (%)	MID change (%)	MRID change (%)	MID change (%)	MRID change (%)	MID change (%)	MRID change (%)	MID change (%)	MRID change (%)
Loma	1.0	25.5	-28.2	10.5	-39.1	20.3	-36.4	13.3	-32.7	11.0	-34.1
	1.2	13.9	-25.7	0.52	-29.2	9.3	-46.1	3.6	-23.6	0.7	-23.0
	1.3	1.4	3.4	-10.2	9.3	-1.9	-3.7	-7.9	13.8	-8.8	15.3
Tabas	1.0	6.3	-30.0	5.5	-21.7	3.0	-43.1	6.1	-36.3	6.7	-22.4
	1.2	9.1	-86.2	9.5	-69.9	8.1	-86.9	9.6	-78.9	11.2	-72.9
	1.5	17.1	-91.5	14.8	-66.7	16.8	-86.2	16.5	-73.7	16.7	-63.2
Northridge	1.0	17.0	-23.1	7.5	-79.3	7.5	-79.3	10.1	-79.8	7.7	-79.6
	1.2	21.2	-81.5	9.5	-73.4	15.7	-81.8	12.9	-81.9	10.1	-74.2
	1.3	22.5	-33.6	12.3	2.4	16.5	-15.5	13.8	-12.9	10.7	5.6
Superstition Hill	1.0	8.9	-46.5	3.5	-63.0	4.6	-53.0	4.8	-58.2	4.5	-59.8
	1.2	14.4	-66.2	4.4	-75.3	9.9	-68.2	4.9	-74.2	5.9	-72.6
	1.5	-3.8	-19.9	-15.5	-72.9	-8.3	-21.9	-11.2	-71.9	-14.9	-71.9
San Fernando	1.0	-5.5	-66.8	-7.0	-69.8	-6.3	-65.4	-4.8	-65.9	-5.4	-70.2
	1.2	-7.2	-86.6	-5.8	-82.9	-7.8	-86.1	-4.3	-84.9	-4.8	-84.5
	1.5	-4.1	-81.5	-5.0	-72.6	-9.1	-87.1	-4.0	-85.6	-3.4	-76.4
Average	1.0	10.4	-38.9	4.0	-54.6	5.8	-55.4	5.9	-54.6	4.9	-53.2
	1.2	10.3	-69.3	3.6	-66.1	7.0	-73.8	5.4	-68.7	4.6	-65.4
	1.3-1.5	6.6	-44.6	-0.7	-40.1	2.8	-42.9	1.4	-46.1	0.1	-38.1
	All	9.1	-50.9	2.3	-53.6	5.2	-57.4	4.2	-56.4	3.2	-52.3

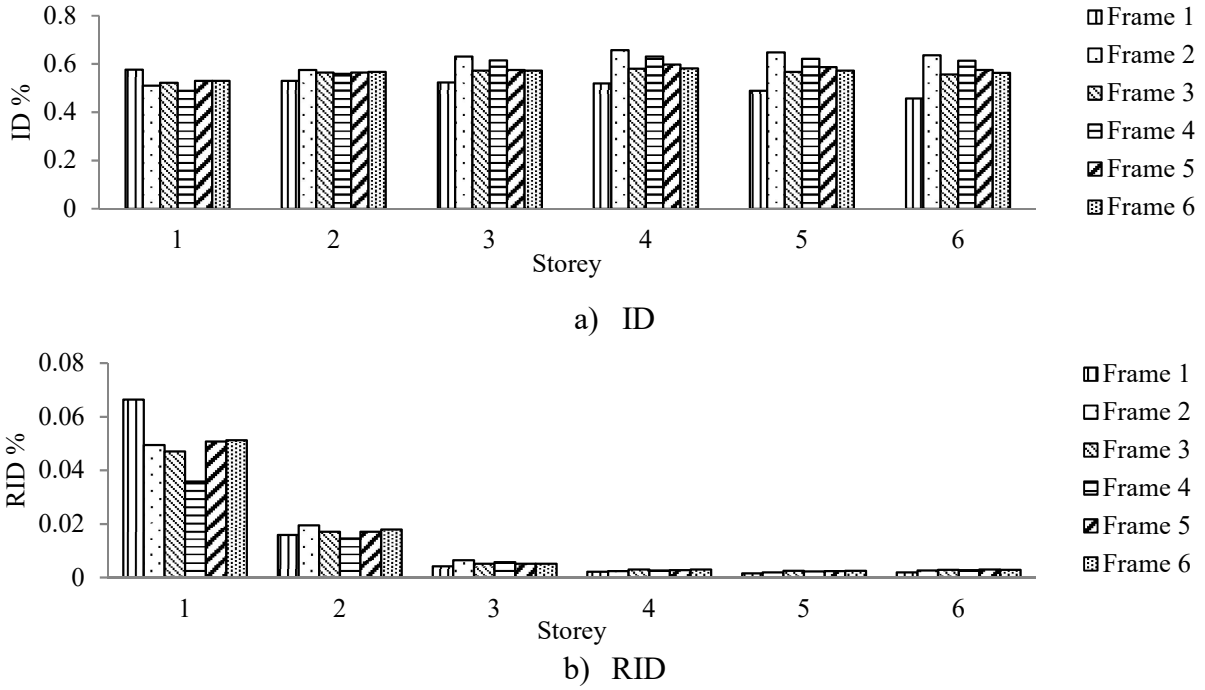

Figure 18: ID and RID distribution considering Loma earthquake at Sa (T1,5%)=1.2g

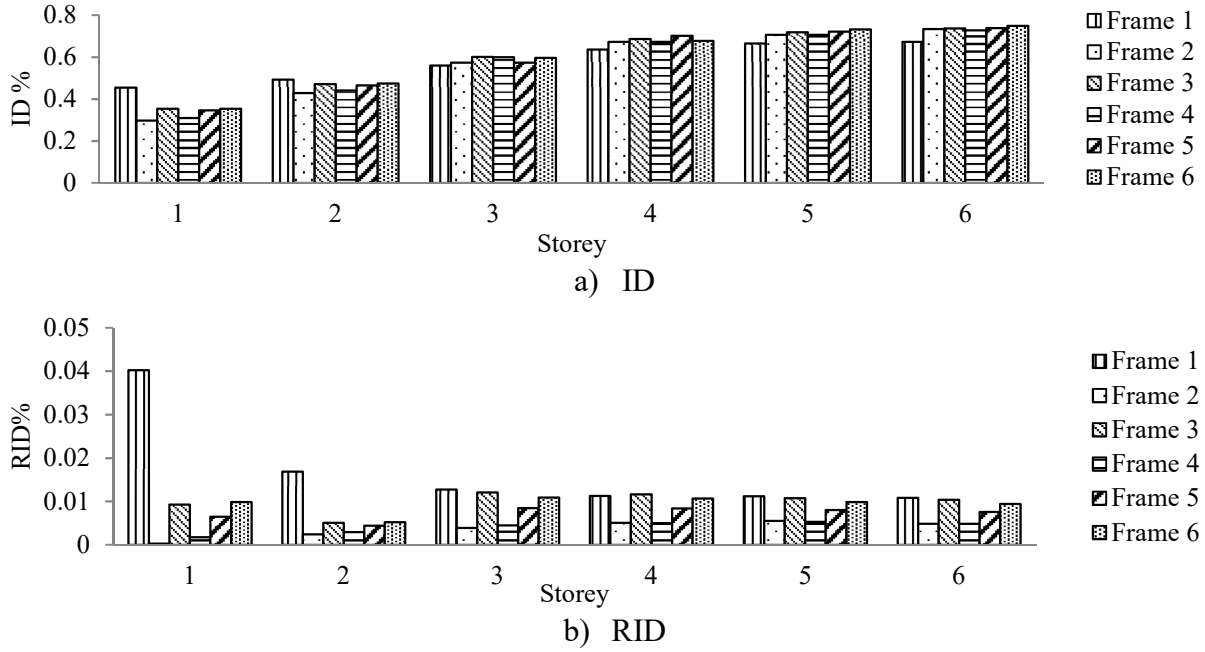

Figure 19: ID and RID distribution due to Tabas earthquake at Sa(T1,5%)=1.2g

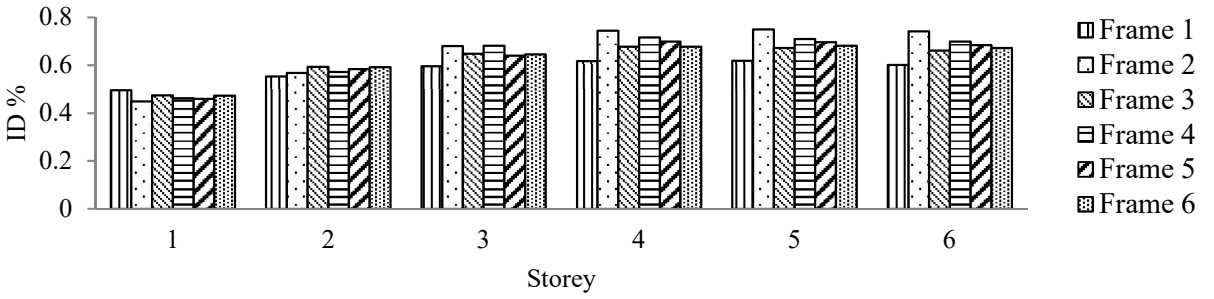

a) ID

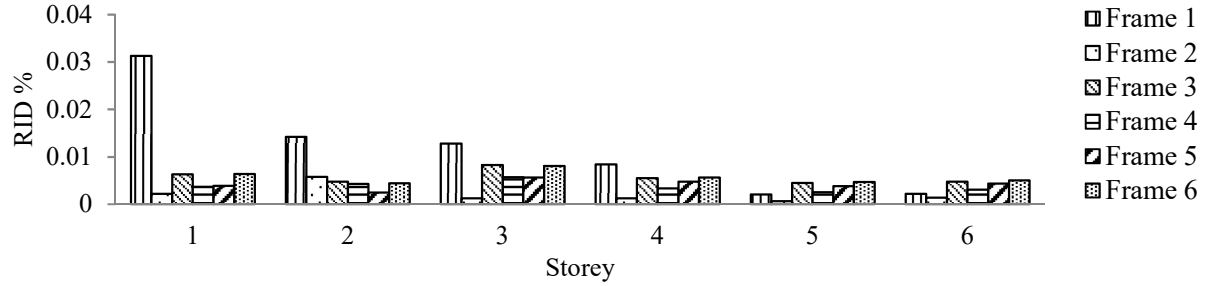

b) RID

Figure 20: ID and RID distribution due to Northridge earthquake at Sa(T1,5%)=1.2g

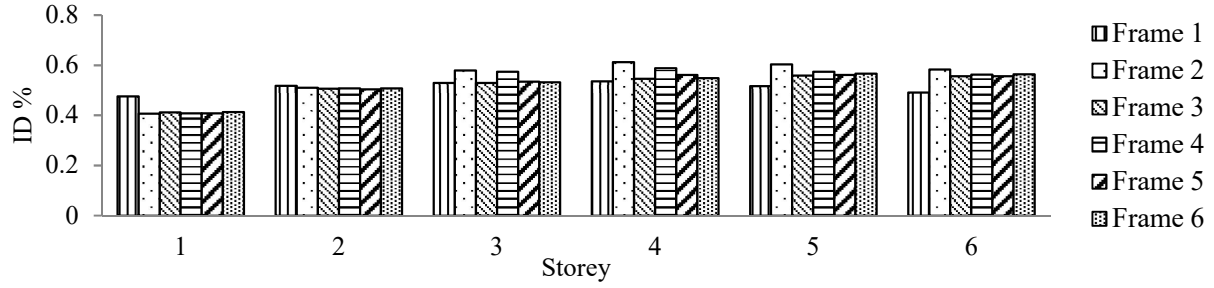

a) ID

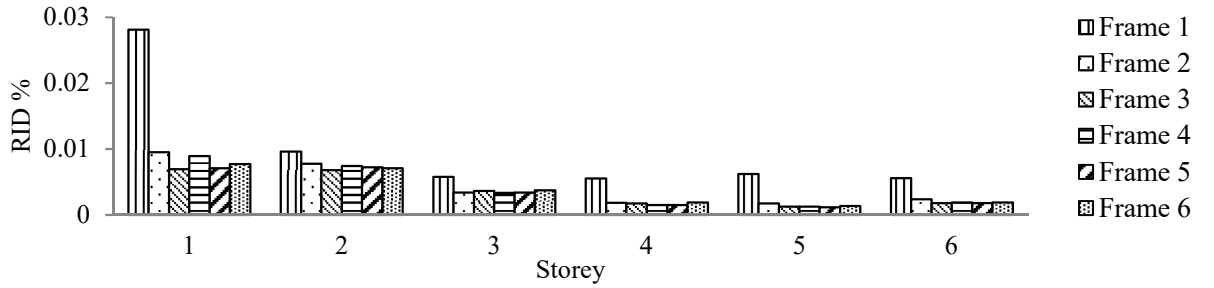

b) RID

Figure 21: ID and RID distribution due to Superstition Hill earthquake at Sa(T1,5%)=1.2g

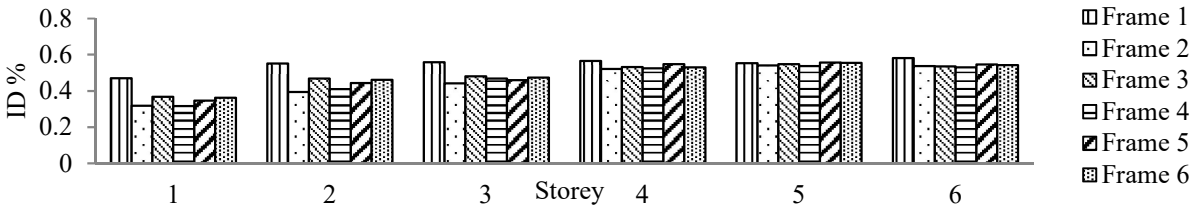

a) ID

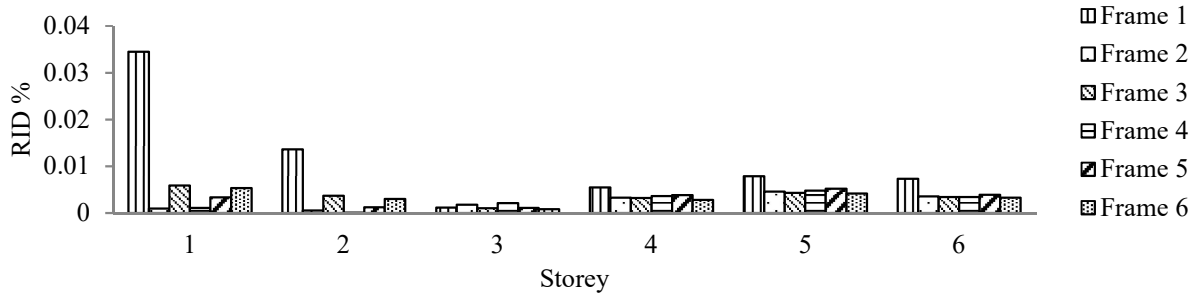

b) RID

Figure 22: ID and RID distribution due to San Fernando earthquake at Sa(T1,5%)=1.2g

Figures 23 to 27 show the damage distribution of the five selected SMA frames. Yielding of the beams of the unbraced bays is observed for all records. All other beams remained elastic. Braces up to fourth stories were yielded while braces of the top two storeys remained elastic. The lowest numbers of yield braces were in Frame 2 due to Tabas and San Fernando records, in Frame 4 due to Loma and Superstition Hill records, and in Frame 5 due to Northridge record. Yielding of columns of SMA frames was observed for the considered earthquakes except San Fernando. A 1st storey column yielded in all frames due to Superstition Hill (1.5g) earthquake and in Frames 2 and 4 due to Loma earthquakes (1.3g). In case of Tabas earthquake (1.5g), yielding of column was observed in the 1st and 5th stories of Frames 3 and 6. Among all SMA frames, Frame 2 experienced

less damage due to Tabas, Northridge, and San Fernando, Frame 3 due to Loma, and Frame 4 due to Superstition Hill earthquakes.

Higher modes of vibrations did not affect the seismic performance of this modular braced frame. This was reflected in the RIDs of Frames 5 and 6 that were similar to Frame 3. RIDs of Frame 4 were better than those for Frame 3, as it reduced the demand on the braces of the first three floors that experienced yielding in majority of the cases. Although SMA connections were between all floors in Frame 2, RIDs of Frames 3, 4, 5, and 6 were lower as inelastic deformations were forced to occur at the locations of the SMA bolts. Considering the cost of SMA materials at one hand and the seismic performance in terms of MID, MRID and damage distribution on the other hand, Frame 4 can be judged as the most suitable solution. Figure 28 compares the rotation of a critical vertical connection of the 1st floor of Frame 4 with that of Frame 1. It is observed that the SMA connections showed excellent recentering capability as compared with the steel connections.

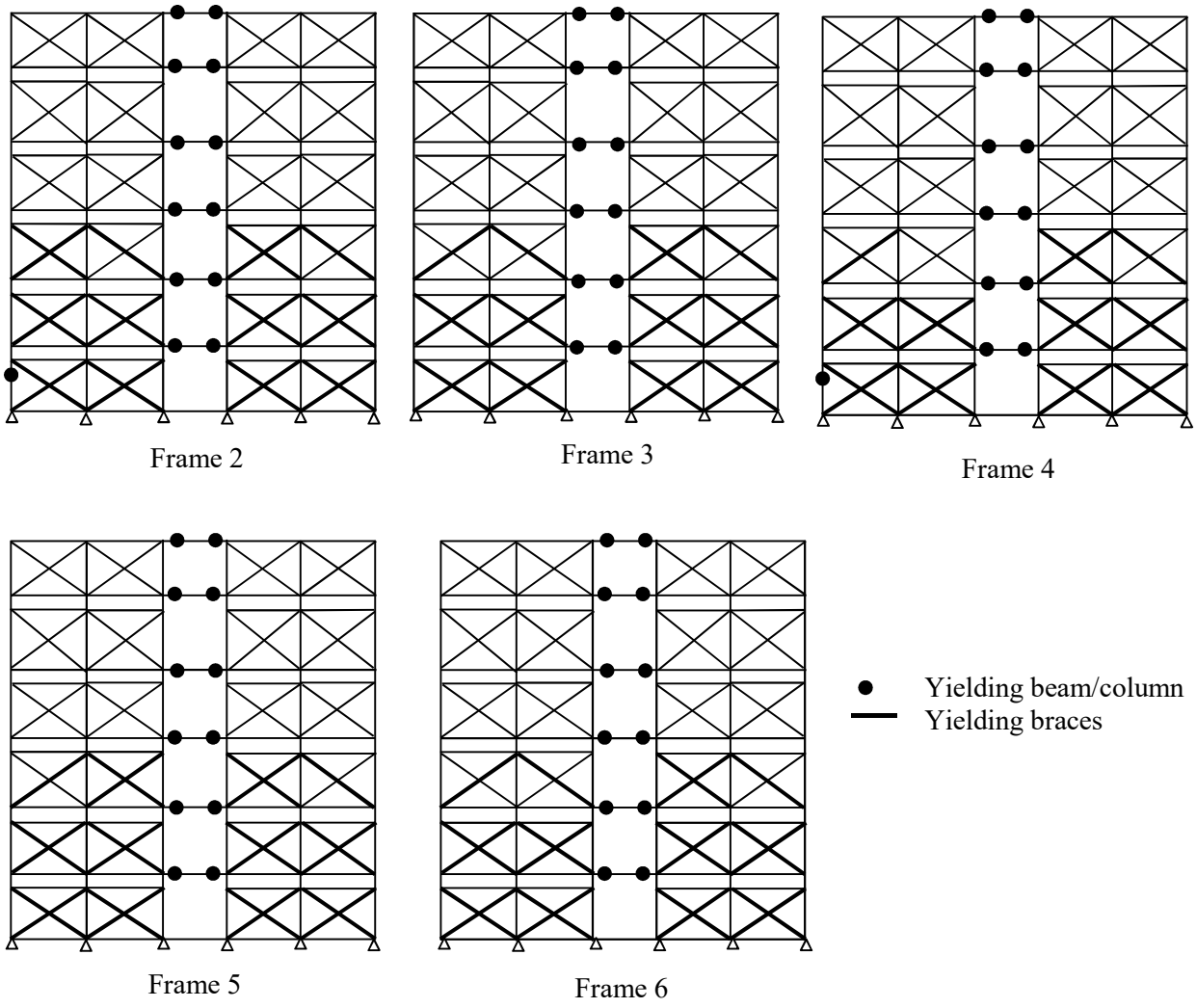

Figure 23: Damage distribution due to Loma earthquake Sa(T1,5%)=1.3g

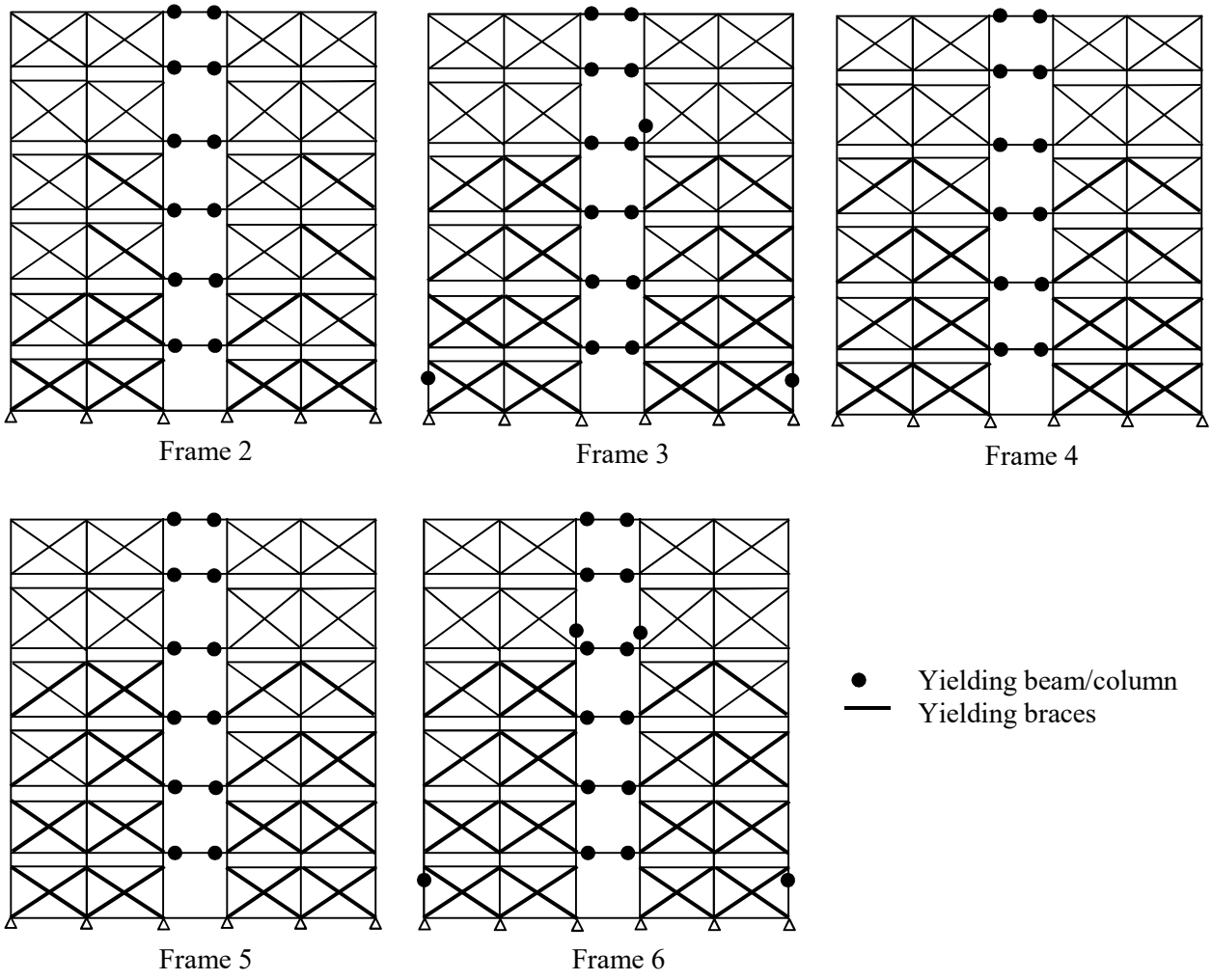

Figure 24: Damage distribution due to Tabas earthquake Sa (T1, 5%) =1.5g

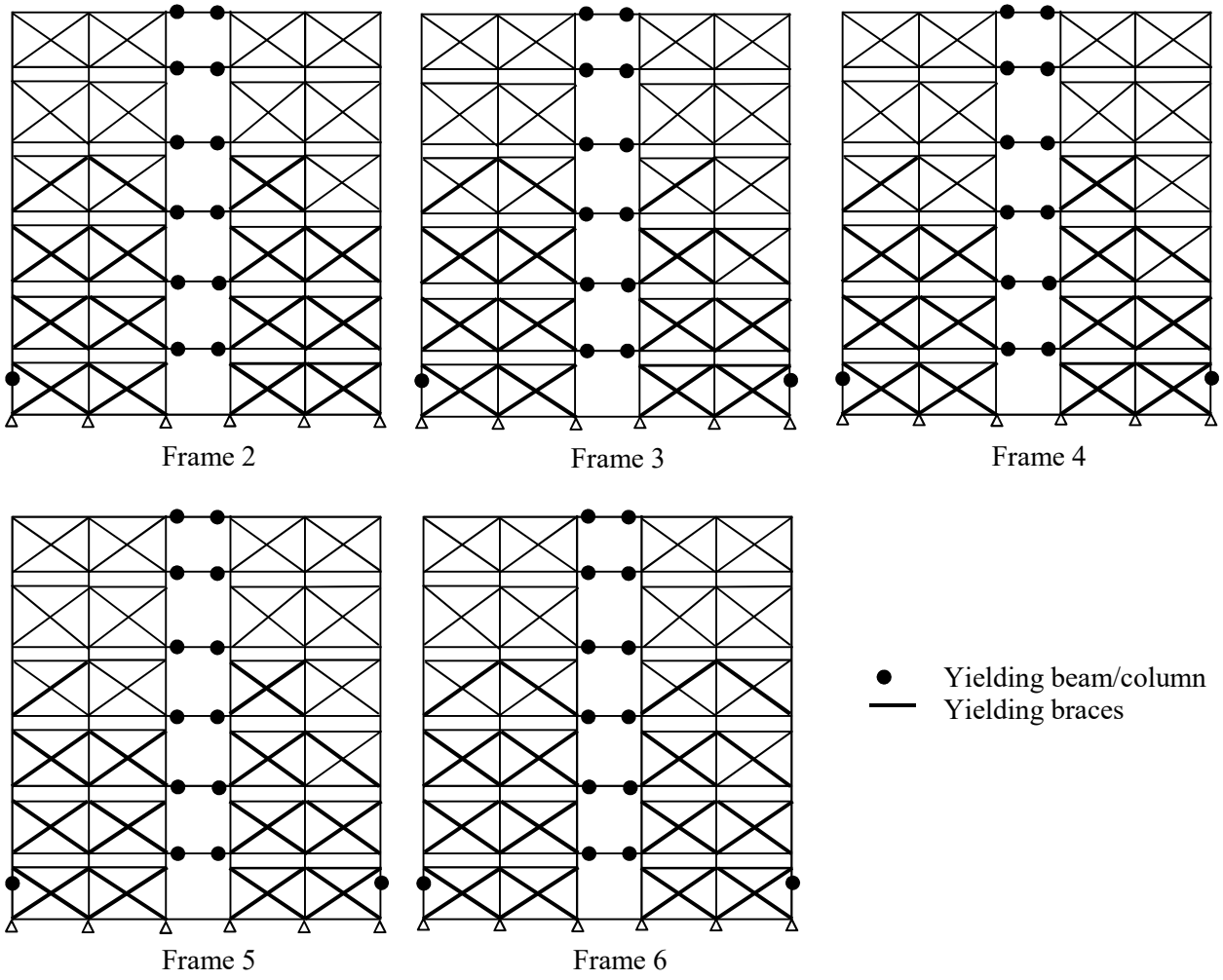

Figure 25: Damage distribution due to Northridge earthquake Sa(T1,5%)=1.3g

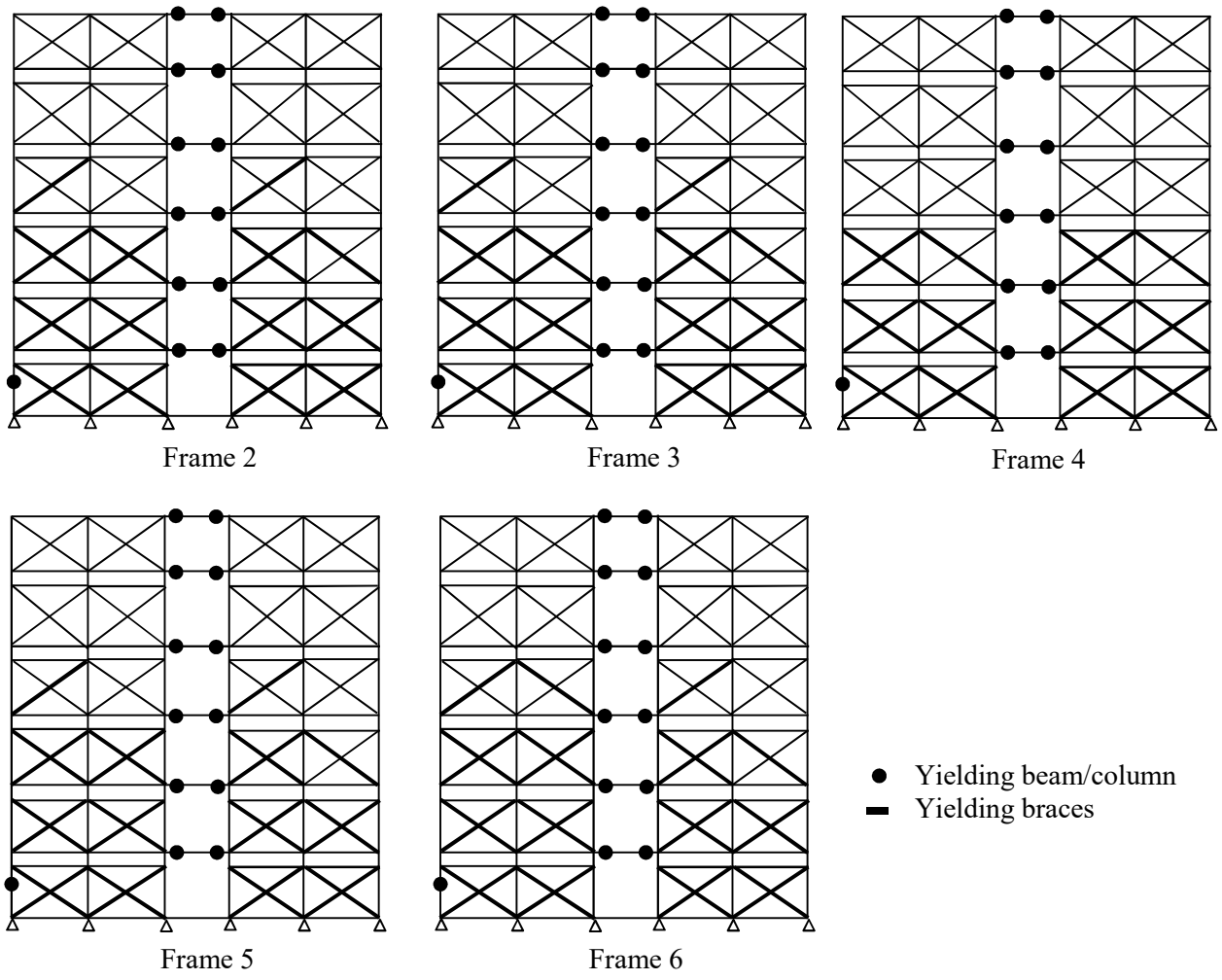

Figure 26: Damage distribution due to Superstition Hills earthquake Sa (T1,5%) =1.5g

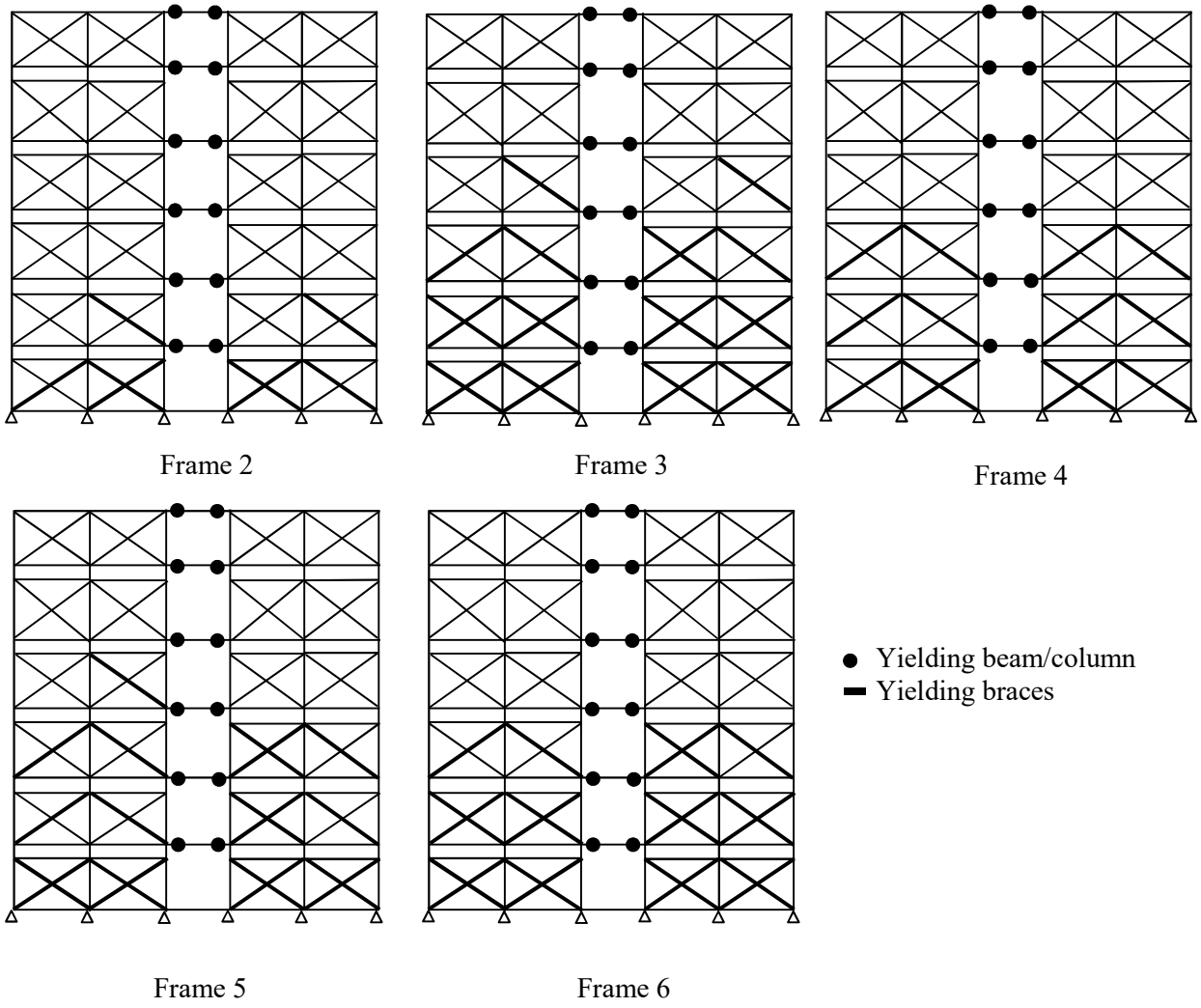

Figure 27: Damage distribution due to San Fernando earthquake Sa (T1,5%) =1.5g

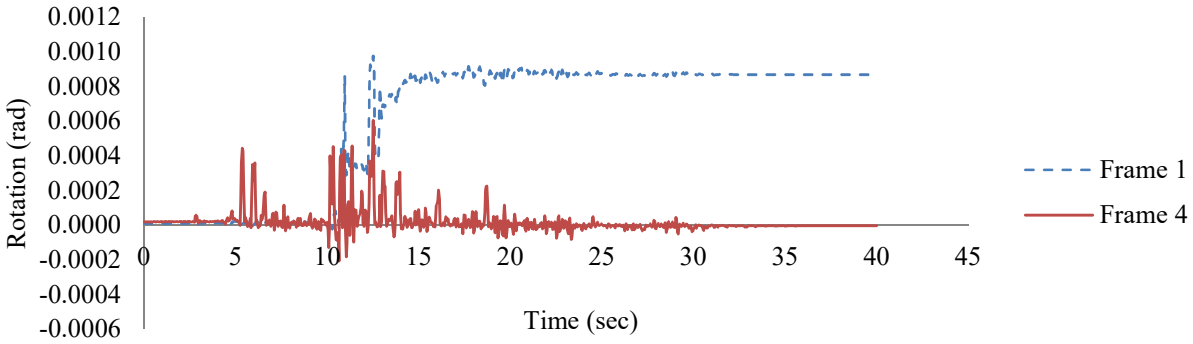

Figure 28: Rotation of vertical connection at first floor due to Tabas earthquake [Sa (T1,5%) =1.5g]

Pushover analysis was conducted for Frame 1 and Frame 4 to further understand the sequence of damage. Figure 29 shows the base shear versus roof displacement and Figure 30 shows the order and distribution of plasticity in both frames. The filled dots represent the yielding of beams, columns or bolts. The brace members drawn in heavier lines have yielded. The numbers associated with the dots and the brace members describe the sequence of yielding. It was observed that yielding of the 1st storey tension braces occurred before yielding of any of the steel bolts in Frame 1. Yielding of tension braces then progressed through the building height. Although some bolts and beams had also yielded, the lateral performance of the frame is mainly governed by yielding of the braces. In case of the SMA frame, the vertical connections are designed in such a way that inelastic deformation occurs mainly at the SMA bolts. Figure 30 confirms that the lateral performance of Frame 4 is governed by the inelastic deformations of the SMA bolts as yielding of the SMA bolts occurred first followed by yielding of braces. This led to reduction in the residual deformations of the frame.

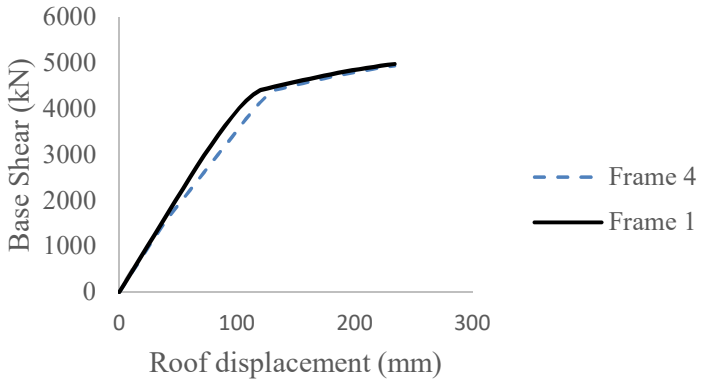

Figure 29: Base shear versus roof displacement

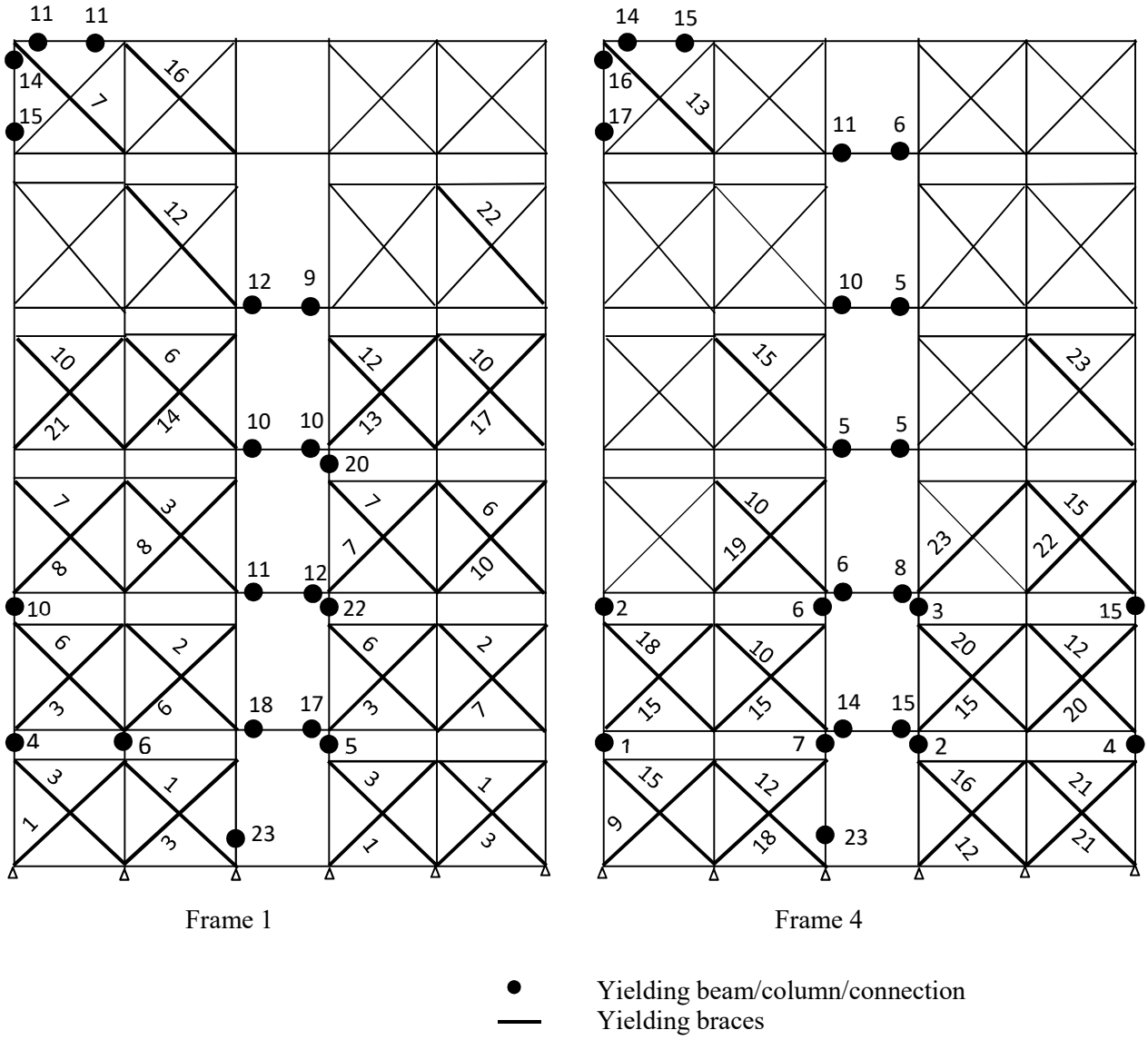

Figure 30: Sequence of yielding

6.0 CONCLUSIONS

The seismic performance of MSBF vertically connected using end plate bolted connections is investigated in this paper in terms of MID, MRID and damage scheme. The connections utilized either high strength steel bolts or superelastic SMA bolts. The use of SMA bolts is aimed at reducing the seismic MRID, which increases with the seismic intensity and following exposure to multiple ground excitations. Finite element models of a MSBF, a bolted beam splice connection

and a beam-column connection utilizing superelastic SMA bars were developed to validate the modeling technique. The modeling technique was then used to model the MSBF connected vertically using end-plate bolted connections. A six-storey building was considered as a case study. IDA of a MSBF vertically connected using high strength steel bolts were performed using five different ground motions scaled to different intensities. The steel bolts were then replaced by superelastic SMA bolts. The SMA bolts provided 40% of the capacity provided by the steel bolts. This ratio is chosen based on preliminary analysis to ensure that the austenite-to-martensite starting stress is reached and the limit for superelastic strains is not exceeded. Five different frames with different SMA locations were selected. Nonlinear dynamic analyses of these frames were conducted using the same records scaled to the same intensities. Specific conclusions from this study are summarised below:

- MSBF connected vertically using end plate steel bolted connections showed good seismic performance in terms of MID, MRID and damage distribution.
- Using SMA connections at the vertical joints between the modules can reduce the residual drifts, and, thus improve the seismic performance of the frame as compared to steel counterpart. The highest reduction is noticed at Sa(T1,5%) of 1.2g. Yielding of the steel braces at higher intensities has decreased this reduction.

- The strains in the SMA bolts did not exceed the superelastic strain limit, which classify the SMA braced frame as self-centered up to collapse.
- Using SMA connections at the vertical joints can increase the MID. This unfavorable effect was reduced at high seismic intensities as yielding of the braces controlled the MID values.

- The values of MID and MRID of MSBFs are influenced by the number and location of the SMA connections, ground motion records and their intensities. Among the SMA frames, Frame 4, where SMA bolts were used in the vertical connections between 1st and 2nd as well as 2nd and 3rd storey modules, showed very good seismic performance compared with the steel frames in terms of MID, MRID and damage schemes. The average overall MID was increased by 5.2% and the average overall MRID was reduced by 57.4%. The demand on the SMA bars, when used at higher stories, was not significant to warrant their use. This was mainly due to the negligible contributions of the higher modes of vibrations and the use of the same vertical connection between all floors. Future research is needed to examine the effect of reducing the capacity of the vertical connection at higher floors on the frame recentering behaviour.
- The seismic performance of the MSBF can be improved by using SMA connections at right locations, which can lead to minor increase in the MID, high reduction in the MRID and better damage distribution. Conclusions of this research are limited to the examined braced modular frame. For other frames and based on research reported in this paper and previous research [27], it is recommended to examine the following cases: using SMA bolts between 1st & 2nd floors, between 1st & 2nd and 2nd & 3rd, and between 1st & 2nd and between floors defining the second mode of vibration. Additional research is needed to examine other frame geometries and develop clear design guidelines for practicing engineers.

REFERENCES

[1] R M Lawson. Building design using modules. Steel Construction Institite (CSI), Publication number 348, UK.

[2] R. M. Lawson, J. Richards, Modular design for high-rise buildings, Proceedings of the Institution of Civil Engineers, Structures and Buildings, 163 (SB3) (2010) 151–164.
[3] C.D. Annan, M.A. Youssef, and M.H. El Naggar, Experimental evaluation of the seismic performance of modular steel-braced frames. Eng. Struct. 31:7(2009a) 1435-1446.
[4] C.D. Annan, M.A. Youssef, M.H. El Naggar. Seismic overstrength in braced frames of modular steel buildings. J. Earthq. Eng. 13(1), (2009b) 1-21.
[5] C.D. Annan, M.A. Youssef, M.H. El Naggar, Seismic vulnerability assessment of modular steel building. J. Earthq. Eng. 13(8) (2009): 1065-1088.
[6] FEMA 350, Recommended seismic design criteria for new steel moment-frame buildings, Federal Emergency Management Agency, 2000.
[7] J.C. Awkar, L. M. Lui, Seismic analysis and response of multistory semirigid frames, Eng. Struct. 21 (1999), 425–441.
[8] E. A. Sumner, T. M. Murray, Behavior of extended end-plate moment connections subject to cyclic loading, J. Struct. Eng. 128:4(2002), 501-508.
[9] J. A. Swanson, R. T. Leon, Bolted steel connections: tests on T-stub components. J. Struct. Eng. 126:1, (2000), 50–56.
[10] J. McCormick, H. Aburano, M. Ikenaga, M. Nakashima. Permissible residual deformation levels for building structures considering both safety and human elements. Proceedings of 14th Conference on Earthquake Engineering, Beijing, China, October 2008.
[11] J. McCormick, J. Tyber, R. DesRoches, k.Gall, H. Maier, Structural engineering with NiTi Part II: Mechanical behavior and scaling, J. Eng. Mech. 133(9) (2007) 1019-1029.
[12] J. Ocel, R. DesRoches, R.T. Leon, W.G. Hess, R. Krumme, J.R. Hayes, S. Sweeney, Steel beam-column connections using shape memory alloys, J. Struct. Eng. 130 (2004) 732–740.
[13] H. Ma, T. Wilkinson, C. Chongdu, Feasibility study on a self-centering beam-to-column connection by using the superelastic behavior of SMAs, Smart. Mater. Struct. 16 (2007) 1555–1563.
[14] H. Ma, M.C.H. Yam, Experimental study on a beam-to-column connection using shape memory alloy, Adv. Mater. Res. 374-377 (2012) 2176-2179.
[15] J. Sepúlveda, R. Boroschek, R. Herrera, O. Moroni, M. Sarrazin, Steel beam-column connection using copper-based shape memory alloy dampers, J. Constr. Steel Res. 64 (2008) 429-435.
[16] M.S. Speicher, R. DesRoches, R.T Leon, Experimental results of a NiTi shape memory alloy (SMA)-based recentering beam-column connection. Eng. Struct. 33 (2011), 2448-2457.
[17] R. DesRoches, B. Taftali, B.R. Ellingwood, Seismic performance assessment of steel frames with shape memory alloy connections, Part I- Analysis and seismic demands, J. Earthq. Eng.14 (2010) 471-486.
[18] P. Sultana, M.A. Youssef, Seismic performance of steel moment resisting frames utilizing superelastic shape memory alloys, J. Constr. Steel. Res. 125 (2016) 239-251.
[19] CAN/CSA-S16-09, Design of Steel Structures, Canadian Standard Association, 2009.
[20] NBCC 2005, National Building Code of Canada.
[21] E.O. Escudero, Comparative Parametric Study on Normal and Buckling Restrained Steel Braces, Master Dissertation, European School of Advanced Studies in Reduction of Seismic Risk, Rose School, Pavia, Italy.

[22] SeismoStruct (version 7) - A computer program for static and dynamic nonlinear analysis of framed structures. Available online from http://www.seismosoft.com.
[23] A.T. Wheeler, M.J. Clarke, G.J. Hancock, Tests of bolted moment end plate connections in tubular members, Proceedings of 14th Australasian Conference on Mechanics of Structures and Materials, University of Tasmania, Hobart, Tasmania, Australia, 331-336, 1995.
[24] E. Auricchio, A. Sacco, one-dimensional model for superelastic shape-memory alloys with different elastic properties between austenite and martensite, Int. J. Nonlin. Mech. 32 (1997) 1101-1114.
[25] D. Fugazza, Shape-memory alloy devices in earthquake engineering: mechanical properties, constitutive modelling and numerical simulations, Master's thesis, European School for Advanced Studies in Reduction of Seismic Risk (ROSE School), Pavia, Italy. 2003.
[26] PEER ground motion database, Pacific Earthquake Engineering Research Center, University of California, Berkeley, USA, 2013, http://ngawest2.berkeley.edu/.
[27] M.A. Youssef, M.A. Elfeki, Seismic Performance of Concrete Frames Reinforced with Superelastic Shape Memory Alloys, Smart Structures and Systems 9(4) (2012) 313-333.